

Search for Quantum Gravity using Astrophysical Neutrino Flavour with IceCube

The IceCube Collaboration

(a complete list of authors can be found at the end of the proceedings)

E-mail: carguelles@g.harvard.edu, k.r.h.farrag@chiba-u.jp,
tepei.katori@kcl.ac.uk

During their long propagation, neutrinos undergo flavour conversions. High-energy astrophysical neutrinos propagate unperturbed over a billion light years in vacuum and are potentially sensitive to small effects caused by new physics. For instance, they are sensitive to the effects of quantum gravity, which are expected to be suppressed by inverse powers of the Planck energy in our low-energy scales. Measuring the coupling of particles to such small effects is difficult via kinematic observables, but could be observable through flavour conversions. Here, we report a recent result from the IceCube Neutrino Observatory, which uses astrophysical neutrino flavours to search for new space-time structure. We found no evidence of anomalous flavour conversion in the IceCube astrophysical neutrino flavour data. Our analysis yielded the most stringent constraint of any known technologies, down to $10^{-42} \text{ GeV}^{-2}$ on dimension-six operators that parametrize the interactions of neutrinos with new fields in vacuum with Bayes factor corresponding to a “strong” rejection.

Corresponding authors: Carlos Argüelles^{1*}, Kareem Farrag², Teppei Katori³

¹ *Harvard University*

² *Chiba University*

³ *King's College London*

* Presenter

The 38th International Cosmic Ray Conference (ICRC2023)
26 July – 3 August, 2023
Nagoya, Japan



1. Introduction

The exploration of quantum gravity (QG) represents a crucial quest in theoretical physics, aiming to reconcile gravity with quantum mechanics and provide a comprehensive understanding of the fundamental interactions of matter and the fabric of space-time. While the Standard Model (SM) of particle physics has successfully described a broad range of phenomena at lower energies, it is considered an effective field theory that awaits an encompassing extension incorporating gravity [1]. The search for QG is difficult since its effects are expected to be suppressed by powers of the Planck energy, $E_P \equiv 1.22 \times 10^{19}$ GeV, which characterizes an energy regime believed to have existed shortly after the Big Bang. However, experimental access to such ultra-high energies is currently beyond the realm of human technological capabilities.

Astrophysical neutrinos, originating from the most energetic astrophysical sources in the universe, provide a unique window to explore phenomena at extreme energy scales. Previous studies have employed astrophysical neutrino spectrum distortion [2] and time-of-flight measurements [3] in attempts to probe QG effects. However, in this contribution, we shift our focus to astrophysical neutrino flavor information and its potential as a probe for QG effects [4]. Neutrino interferometry, a technique previously employed by the IceCube Neutrino Observatory [4], offers a promising avenue to investigate the presence of QG effects. By studying the relative amounts of neutrino flavors, it provides a means to uncover deviations from the expected behavior predicted by the Standard Model. Despite extensive efforts, no evidence of QG has been observed in previous neutrino interferometry experiments [5]. Notably, the unique advantage of studying astrophysical neutrinos lies in their higher energies and longer propagation distances [6], leading to an enhanced sensitivity in probing potential QG effects [7].

In this contribution, we report the results of a search for QG effects using data collected by the IceCube Neutrino Observatory [8] over 7.5 years in the High-Energy Starting Event (HESE) selection [9]. For this analysis we use the ternary classification method described in Ref. [10], which include the observation of the first two astrophysical tau neutrinos candidates. Our search parametrizes the effect of QG using effective operators introduced in Ref. [7] and reports upper limits on each of the operators' coefficients.

2. Formalism and Methodology

One of the potential consequences of QG at low, sub-Planckian energy scales is spontaneous breaking of Lorentz symmetry. The breakage of Lorentz symmetry can be parametrized at low, sub-Planckian energies by introducing a field in vacuum that does not transform according to the Lorentz transformation, but instead has a particular space-time orientation [11]. The interaction of this field with neutrinos can be due to, both, renormalizable and non-renormalizable operators, where the latter are expected to be suppressed by the Planck energy. Since the interaction of this field with the neutrinos depends on the precise theory of QG, we take a pragmatic approach and parametrize the interactions of neutrinos with this field by effective operators as introduced in Refs. [7, 11], where we only consider the time-like component of the field.

The potential interactions between this field and the neutrinos modify the neutrino energy in a potentially flavor-dependent manner. Referring to the notation of the effective operators provided

in Ref. [4], the Hamiltonian governing neutrino evolution, Eq. (1), can be expressed as follows,

$$H = U \frac{m^2}{2E} U^\dagger + \begin{pmatrix} \overset{\circ}{a}_{ee}^{(3)} & \overset{\circ}{a}_{e\mu}^{(3)} & \overset{\circ}{a}_{\tau e}^{(3)} \\ \overset{\circ}{a}_{e\mu}^{(3)*} & \overset{\circ}{a}_{\mu\mu}^{(3)} & \overset{\circ}{a}_{\mu\tau}^{(3)} \\ \overset{\circ}{a}_{\tau e}^{(3)*} & \overset{\circ}{a}_{\mu\tau}^{(3)*} & \overset{\circ}{a}_{\tau\tau}^{(3)} \end{pmatrix} - E \cdot \begin{pmatrix} \overset{\circ}{c}_{ee}^{(4)} & \overset{\circ}{c}_{e\mu}^{(4)} & \overset{\circ}{c}_{\tau e}^{(4)} \\ \overset{\circ}{c}_{e\mu}^{(4)*} & \overset{\circ}{c}_{\mu\mu}^{(4)} & \overset{\circ}{c}_{\mu\tau}^{(4)} \\ \overset{\circ}{c}_{\tau e}^{(4)*} & \overset{\circ}{c}_{\mu\tau}^{(4)*} & \overset{\circ}{c}_{\tau\tau}^{(4)} \end{pmatrix} + \dots \quad (1)$$

Here, U denotes the neutral-lepton mixing matrix, E the energy in the laboratory frame, m^2 represents the diagonal matrix containing the eigenvalues of neutrino masses, and the ellipsis represents a series of higher-order terms with alternating signs and increasing power in energy.

In addition to the standard first term, there are two sets of new coefficients: the CPT -odd terms ($\overset{\circ}{a}^{(3)}$, $\overset{\circ}{a}^{(5)}$, $\overset{\circ}{a}^{(7)}$, ...) and the CPT -even terms ($\overset{\circ}{c}^{(4)}$, $\overset{\circ}{c}^{(6)}$, $\overset{\circ}{c}^{(8)}$, ...). The sign conventions follow those of the Standard-Model Extension (SME) as described in Ref. [11]. The integers in parentheses represent the dimensions, denoted as d , of each operator. Consequently, the units of these operators are GeV^{4-d} .

The dimension-three and dimension-four operators are renormalizable, while all other operators are non-renormalizable. All effective operators that influence neutrino flavor conversions possess Lorentz indices with temporal, spatial, and mixed components in the Sun-centered celestial equatorial frame (SCCEF) [5]. However, the astrophysical neutrino flux assumed in this analysis pertains to the diffuse flux. The incoming neutrino directions are uniformly distributed as a consequence of this. This averaging process nullifies any spatial effects, rendering this analysis only sensitive to the isotropic coefficients. This is indicated in our notation by the circles placed above the operators, signifying their spatial isotropy.

In general, two or more operators with different dimensions (such as $\overset{\circ}{a}_{ee}^{(3)}$ and $\overset{\circ}{c}_{ee}^{(4)}$) may simultaneously affect the astrophysical neutrino flavor ratio. However, for this scenario to be relevant, it would require the operators to have similar relative sizes within the energy range considered in this analysis. We regard this as an unlikely coincidence and, therefore, do not make this assumption in our study.

To simplify this analysis, we take only one of the operators to be non-vanishing when presenting our results. Alternatively, it is also possible to consider two elements from the same dimensional operator, such as $\overset{\circ}{a}_{ee}^{(3)}$ and $\overset{\circ}{a}_{e\mu}^{(3)}$. Since all these elements are complex numbers, it is feasible to establish limits for both the real and imaginary parts, such as for the scenario of $\text{Re}(\overset{\circ}{a}_{ee}^{(3)})$ and $\text{Im}(\overset{\circ}{a}_{ee}^{(3)})$. Nevertheless, the available data statistics do not permit simultaneous fitting of two operators with identical energy dimensions.

Furthermore, the data sample comprises a combination of neutrinos and antineutrinos, and it is not possible to distinguish them on an event-by-event basis using the reconstructions employed in this analysis. To evaluate the influence of the neutrino-to-antineutrino ratio, we performed tests by fitting neutrino-only and antineutrino-only scenarios using Monte Carlo simulations. The results of these tests demonstrated only marginal changes to the results. Specifically, it was observed that the complex phase had a minor impact on the limits. Consequently, in this analysis, we focus on searching for one non-negative real element of each operator individually. For comprehensive constraints and a more detailed discussion on the complex phases, we encourage readers to refer to [4].

The introduction of new physics operators, such as $\overset{\circ}{a}^{(3)}$, $\overset{\circ}{c}^{(4)}$, $\overset{\circ}{a}^{(5)}$, $\overset{\circ}{c}^{(6)}$, and so on, leads to modifications in the vacuum through new interactions. These modifications are reflected in the

mixing matrix element, $V_{\alpha i}(E)$, which can be determined through neutrino mixing. The quantity of interest is the neutrino flux of flavor β at Earth, denoted as $\phi_{\beta}^{\oplus}(E)$, rather than the neutrino mixing itself. It is important to note that the composition of the flux at Earth is also influenced by the initial neutrino flux of flavor α at the source, denoted as $\phi_{\alpha}^i(E)$ [12]. Additionally, due to the limited number of astrophysical neutrinos available, we are constrained to using the energy-averaged flavor composition,

$$\bar{\phi}_{\beta}^{\oplus} = \frac{1}{|\Delta E|} \int_{\Delta E} \sum_{\alpha} \bar{P}_{\nu_{\alpha} \rightarrow \nu_{\beta}}(E) \phi_{\alpha}^i(E) dE, \quad (2)$$

where we assume a single power-law spectrum for the flux of astrophysical neutrinos at production. By integrating over this spectrum, and normalizing the calculated flavor ratio, this yields the expected terrestrial neutrino flavor composition, f_{β}^{\oplus} :

$$f_{\beta}^{\oplus} = \bar{\phi}_{\beta}^{\oplus} / \sum_{\gamma} \bar{\phi}_{\gamma}^{\oplus}. \quad (3)$$

By diagonalizing Hamiltonian (Eq. (1)) we compute the flavor ratio via the method described in Ref. [7]. Initially, neutrino flavor eigenstates $|\nu_{\alpha}\rangle$ can be described by the superposition of Hamiltonian eigenstates, $|\nu_i\rangle$,

$$|\nu_{\alpha}\rangle = \sum_i V_{\alpha i}(E) |\nu_i\rangle. \quad (4)$$

Here, $V_{\alpha i}(E)$ denotes the effective mixing of neutrinos including the contribution from the new physics operator (Eq. (1)). Considering the extensive baselines covered and the high energies involved, the resulting oscillation frequencies of neutrinos are significantly higher and are smoothed out by the detector's energy resolution. In this regime, the transition probability of neutrinos for any given energy E can be expressed purely in terms of a function of $V_{\alpha i}(E)$. Specifically, we find

$$P_{\nu_{\alpha} \rightarrow \nu_{\beta}}(E) = \sum_i |V_{\alpha i}(E)|^2 |V_{\beta i}(E)|^2, \quad (5)$$

where the sum encompasses all possible eigenstates. Example of resulting trajectories for given standard source flavor compositions are illustrated in Fig. 1. Note that in the limit of vanishing QG effects, V becomes the PMNS matrix, U , and the standard astrophysical neutrino flavor composition is recovered. This can be seen in Fig. 1 by the fact that all lines start in the standard bow-tie-shaped region in the center of the triangle.

In this analysis, a total of fourteen nuisance parameters representing systematic errors are simultaneously constrained. Firstly, we consider six oscillation parameters [15]: two neutrino mass-square differences, $\Delta m_{21}^2 = 7.42_{-0.20}^{+0.21}$ (in units of 10^{-5} eV^2), $\Delta m_{31}^2 = 2.514_{-0.027}^{+0.028}$ (in units of 10^{-3} eV^2); three mixing angles, $\sin^2 \theta_{12} = 0.304_{-0.012}^{+0.013}$, $\sin^2 \theta_{23} = 0.570_{-0.024}^{+0.018}$, and $\sin^2 \theta_{31} = 0.02221_{-0.00062}^{+0.00068}$; and the Dirac CP -violating phase, δ_{CP} (unconstrained).

Secondly, we consider five flux systematics, which can be classified into two categories: normalisation of each flux component and spectral index assuming a single power law. The normalisation systematic errors are introduced as shifts from the nominal predictions, including the astrophysical neutrino flux (Φ_{astro} , unconstrained), atmospheric neutrino conventional flux (Φ_{conv} , 40% uncertainty), prompt flux (Φ_{prompt} , unconstrained), and atmospheric muon flux (Φ_{muon} , 50%

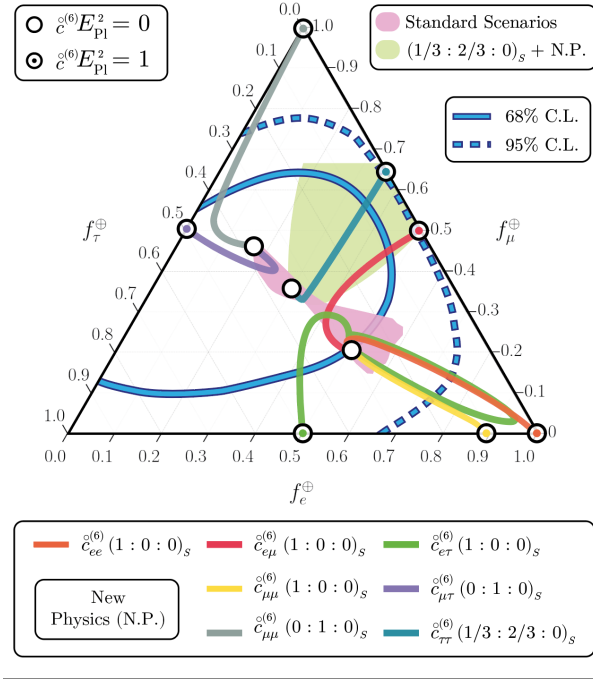


Figure 1: Flavor trajectories. The anticipated flavor composition at Earth is depicted for the Standard Model with standard neutrino oscillations [13] (depicted as a light-pink, bow-tie-shaped region), the region permitted by unitarity constraints considering pion production [14] (presented as a pastel-green pentagonal-like shape), and for various operators representing distinct initial flavor compositions and flavor textures.

uncertainty). The astrophysical neutrino spectral index (γ_{astro} , unconstrained) is also included as a systematic error, with a best-fit value similar to a dedicated study of the same sample [9].

Furthermore, we introduce three detector systematic parameters: the Digital Optical Module (DOM) [8] overall efficiency (ϵ_{DOM} , 10% uncertainty), DOM angular dependence ($\epsilon_{\text{head-on}}$, 50% uncertainty), and the in-ice photon propagation anisotropy around DOMs (a_s , 20% uncertainty).

Additional systematic errors arising from the modeling of atmospheric neutrinos and cosmic rays are considered in other analyses [9?]. However, these systematics are not taken into account in this analysis because they mainly affect low-energy events (less than 100 TeV). The QG-motivated physics limit we set depends on the highest tail of the event distribution.

Finally, the data and the Monte Carlo expectation are compared using the likelihood introduced in Ref. [16], which takes into account errors resulting from the finite size of the Monte Carlo sample.

To determine our limits, we employ two independent analysis methods based on frequentist and Bayesian approaches [17]. The Bayesian approach is chosen as the official result of this analysis, while the faster frequentist approach is used to validate the Bayesian results. The reason for this choice is that it is too computationally expensive to produce a trials-calibrated frequentist result and thus we decided to fall-back to a proper Bayesian prescription. Both methods utilize the same 15-dimensional likelihood function with 14 systematic errors, where one parameter represents a new physics scale.

In the Bayesian case, the evidence is obtained by marginalising the likelihood over the systematic parameters using nested sampling, assuming model priors from Ref. [9]. We employ

the MultiNest algorithm [18] with 800 live points, approximately $\sim 18,000$ steps, and a tolerance of 0.05. We perform nearly $\sim 200,000$ similar calculations with different configurations to explore the parameter phase space and identify the signal. An example of a posterior distribution from one configuration is shown in the Supplemental Information ¹ of Ref. [19].

Next, we define the Bayes Factor (BF) as the ratio of the model evidence to the null hypothesis, which assumes no QG effects. We utilize Jeffreys' scale to establish substantial and strong limits, which are defined by the BF being greater than 10 (substantial limit) and 31.6 (strong limit). The Supplementary Information published in Ref. [19] provides substantial and strong limits from this procedure for selected source flavor ratio assumptions. We repeat this construction of BFs with different source flavor compositions ($x : 1 - x : 0$), allowing us to construct limits as a function of source flavor ratio x (Fig. 2). We then spline to extrapolate values between the set of all BFs for given x and smooth the resulting limit. This procedure is then repeated for each dimension between dimensions three and eight.

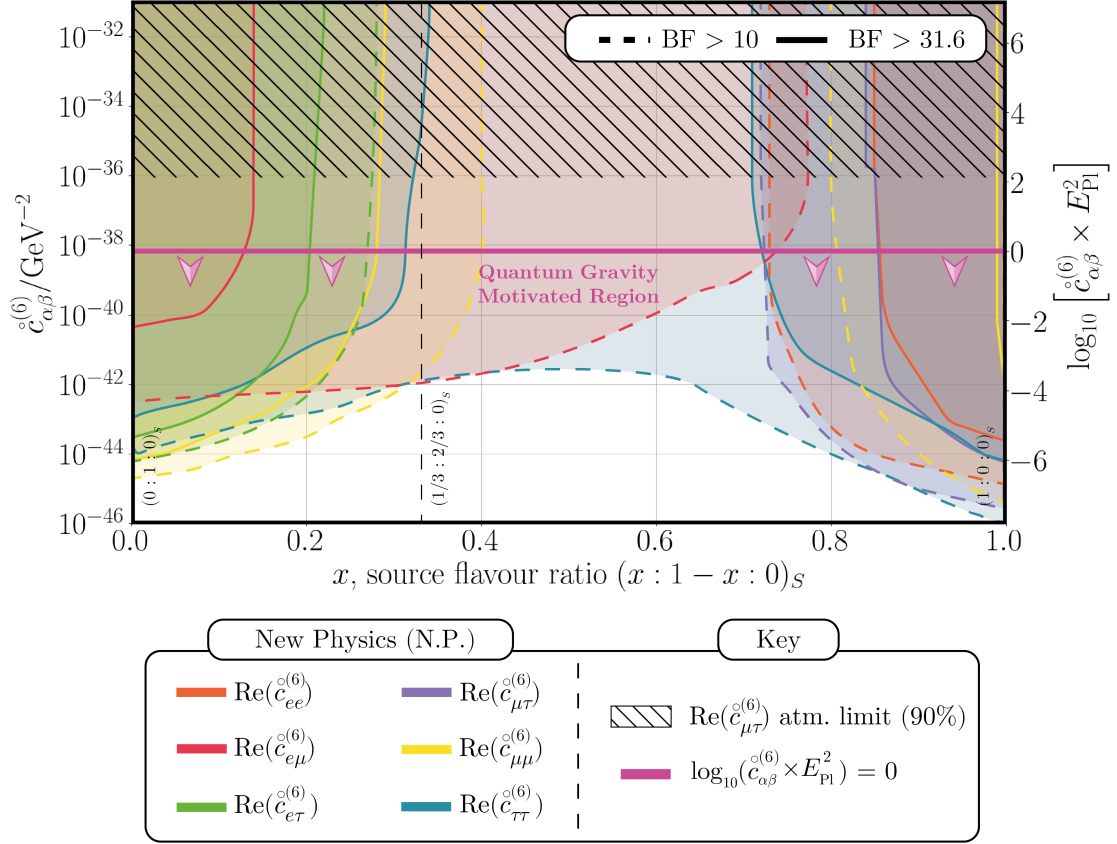
The limits obtained in this analysis become stronger for higher dimensions due to the enhanced energy dependence described by Eq. (1). As the dimension increases, the limits from astrophysical neutrino interferometry become significantly more stringent compared to those from atmospheric neutrino interferometry. However, for dimension seven and eight operators, QG-motivated physics is expected to be smaller than E_P^{-3} and E_P^{-4} , respectively. Consequently, this analysis lacks sensitivity to operators of such sizes. It should be noted that the dimension-three and -four operators are renormalizable, and thus the definition of QG-motivated physics does not apply in the same manner.

3. Results

The main results of this work are shown for dimension-six operators in Fig. 2, other constraints can be found in the Supplemental Material in Ref. [19].

The constraints depend on the assumed flavor composition at the source and the flavor-texture of the interaction. As can be seen in the figure for several combination of these two parameters the constraints obtained surpass the Planck scale: we have entered the QG regime. This implies that this technique has significant potential to reach this scale and will improve as our understanding of astrophysical sources evolves. One notable point is that the $\hat{c}_{\tau\tau}^{(d)}$ coefficient is constrained beyond the Planck scale for all possible choices of the source flavor ratio at substantial level. Large values of this coefficient suppress the transition from muon and electron neutrinos to tau neutrinos, thus, to first order, a non-zero value of this coefficient is constrained to the level that a non-tau astrophysical component is ruled out. Additionally, for the pion production mechanism, which is present in many astrophysical neutrino production scenarios, the $\hat{c}_{e\mu}^{(d)}$ and $\hat{c}_{\mu\mu}^{(d)}$ operators are constrained to the substantial level. For muon-damped scenarios, where we expected only muon neutrinos at the source, the constraints at the strong-level beyond the Planck scale are obtained for $\hat{c}_{\tau\tau}^{(d)}$, $\hat{c}_{\mu\tau}^{(d)}$, $\hat{c}_{\mu\mu}^{(d)}$, $\hat{c}_{e\mu}^{(d)}$, and $\hat{c}_{e\tau}^{(d)}$.

¹<https://www.nature.com/articles/s41567-022-01762-1/figures/4>



5 **Figure 2: Constraints on dimension-six effective operators as a function of the initial flavor composition.**
 6 The hashed region The hashed region on top corresponds to the constraint obtained using atmospheric
 7 neutrinos [4]. The shaded regions correspond to constrained regions where the solid edges demarcate the BF
 8 for strong constraint, while the dashed-edges delineate the substantial limit. Where substantial corresponds
 9 to a BF of 10, while strong is given by 31.6 according to Jeffrey’s scale.

4. Conclusion

Here, we have reported results for the first search for QG effects using astrophysical neutrino flavors. Though these have been expressed as constraints on Lorentz-violating operators, they are constraints on the size of any flavor-non-trivial potential that may permeate space. Thus, some of the constraints derived in this work translate directly to other scenarios such as long-range forces, neutrino-dark matter interactions, among others; see Ref. [20] and references therein.

The constraints obtained in this work are limited by our capacity to reconstruct neutrino flavor ratios, which is expected to improve with better characterization of the Antarctic ice [21] and reconstruction techniques [22–24], and by the limited sample size of astrophysical neutrinos [25, 26]. We expect that future follow-up analyses will pierce deeply into the QG-motivated regime.

References

- [1] S. Weinberg *Phys. Rev. Lett.* **19** (1967) 1264–1266.
- [2] J. S. Diaz, A. Kostelecky, and M. Mewes *Phys. Rev. D* **89** no. 4, (2014) 043005.
- [3] J. Ellis, N. E. Mavromatos, A. S. Sakharov, and E. K. Sarkisyan-Grinbaum *Phys. Lett. B* **789** (2019) 352–355.
- [4] **IceCube** Collaboration, M. G. Aartsen *et al.* *Nature Phys.* **14** no. 9, (2018) 961–966.
- [5] V. A. Kostelecky and N. Russell *Rev. Mod. Phys.* **83** (2011) 11–31.
- [6] C. A. Argüelles, M. Bustamante, A. Kheirandish, S. Palomares-Ruiz, J. Salvado, and A. C. Vincent *PoS ICRC2019* (2020) 849.
- [7] C. A. Argüelles, T. Katori, and J. Salvado *Phys. Rev. Lett.* **115** (2015) 161303.
- [8] **IceCube** Collaboration, M. G. Aartsen *et al.* *JINST* **12** no. 03, (2017) P03012.
- [9] **IceCube** Collaboration, R. Abbasi *et al.* *Phys. Rev. D* **104** (2021) 022002.
- [10] **IceCube** Collaboration, R. Abbasi *et al.* *Eur. Phys. J. C* **82** no. 11, (2022) 1031.
- [11] A. Kostelecky and M. Mewes *Phys. Rev. D* **85** (2012) 096005.
- [12] M. Bustamante, J. F. Beacom, and W. Winter *Phys. Rev. Lett.* **115** no. 16, (2015) 161302.
- [13] N. Song, S. W. Li, C. A. Argüelles, M. Bustamante, and A. C. Vincent *JCAP* **04** (2021) 054.
- [14] M. Ahlers, M. Bustamante, and S. Mu *Phys. Rev. D* **98** no. 12, (2018) 123023.
- [15] I. Esteban, M. C. Gonzalez-Garcia, M. Maltoni, T. Schwetz, and A. Zhou *JHEP* **09** (2020) 178.
- [16] C. A. Argüelles, A. Schneider, and T. Yuan *JHEP* **06** (2019) 030.
- [17] S. Mandalia, *Searching for Quantum Gravity with Neutrinos, Optical Module Beam Test at Fermilab and Hadronization Model studies for IceCube*. PhD thesis, Queen Mary, U. of London (main), 2020.
- [18] F. Feroz, M. P. Hobson, and M. Bridges *Mon. Not. Roy. Astron. Soc.* **398** (2009) 1601–1614.
- [19] **IceCube** Collaboration, R. Abbasi *et al.* *Nature Phys.* **18** no. 11, (2022) 1287–1292.
- [20] C. A. Argüelles *et al.* *Eur. Phys. J. C* **83** no. 1, (2023) 15.
- [21] **IceCube** Collaboration, A. Ishihara *PoS ICRC2019* (2021) 1031.
- [22] **IceCube** Collaboration, F. Bradascio and T. Glüsenskamp *PoS ICRC2019* (2021) 846.
- [23] R. Abbasi *et al.* *JINST* **16** (2021) P07041.
- [24] F. J. Yu, J. Lazar, and C. A. Argüelles *arXiv* (2023) 2303.08812.
- [25] M. Ackermann *et al.* *JHEAp* **36** (2022) 55–110.
- [26] R. Mammen Abraham *et al.* *J. Phys. G* **49** no. 11, (2022) 110501.

Full Author List: IceCube Collaboration

R. Abbasi¹⁷, M. Ackermann⁶³, J. Adams¹⁸, S. K. Agarwalla^{40, 64}, J. A. Aguilar¹², M. Ahlers²², J.M. Alameddine²³, N. M. Amin⁴⁴, K. Andeen⁴², G. Anton²⁶, C. Argüelles¹⁴, Y. Ashida⁵³, S. Athanasiadou⁶³, S. N. Axani⁴⁴, X. Bai⁵⁰, A. Balagopal V.⁴⁰, M. Baricevic⁴⁰, S. W. Barwick³⁰, V. Basu⁴⁰, R. Bay⁸, J. J. Beatty^{20, 21}, J. Becker Tjus^{11, 65}, J. Beise⁶¹, C. Bellenghi²⁷, C. Benning¹, S. BenZvi⁵², D. Berley¹⁹, E. Bernardini⁴⁸, D. Z. Besson³⁶, E. Blaufuss¹⁹, S. Blot⁶³, F. Bontempo³¹, J. Y. Book¹⁴, C. Boscolo Meneguolo⁴⁸, S. Böser⁴¹, O. Botner⁶¹, J. Böttcher¹, E. Bourbeau²², J. Braun⁴⁰, B. Brinson⁶, J. Brostean-Kaiser⁶³, R. T. Burley², R. S. Busse⁴³, D. Butterfield⁴⁰, M. A. Campana⁴⁹, K. Carloni¹⁴, E. G. Carnie-Bronca², S. Chattopadhyay^{40, 64}, N. Chau¹², C. Chen⁶, Z. Chen⁵⁵, D. Chirkin⁴⁰, S. Choi⁵⁶, B. A. Clark¹⁹, L. Classen⁴³, A. Coleman⁶¹, G. H. Collin¹⁵, A. Connolly^{20, 21}, J. M. Conrad¹⁵, P. Coppin¹³, P. Correa¹³, D. F. Cowen^{59, 60}, P. Dave⁶, C. De Clercq¹³, J. J. DeLaunay⁵⁸, D. Delgado¹⁴, S. Deng¹, K. Deoskar⁵⁴, A. Desai⁴⁰, P. Desati⁴⁰, K. D. de Vries¹³, G. de Wasseige³⁷, T. DeYoung²⁴, A. Diaz¹⁵, J. C. Díaz-Vélez⁴⁰, M. Dittmer⁴³, A. Domi²⁶, H. Dujmovic⁴⁰, M. A. DuVernois⁴⁰, T. Ehrhardt⁴¹, P. Eller²⁷, E. Ellinger⁶², S. El Mentawi¹, D. Elsässer²³, R. Engel^{31, 32}, H. Erpenbeck⁴⁰, J. Evans¹⁹, P. A. Evenson⁴⁴, K. L. Fan¹⁹, K. Fang⁴⁰, K. Farrag¹⁶, A. R. Fazely⁷, A. Fedynitch⁵⁷, N. Feigl¹⁰, S. Fiedlschuster²⁶, C. Finley⁵⁴, L. Fischer⁶³, D. Fox⁵⁹, A. Frankowiak¹¹, A. Fritz⁴¹, P. Fürst¹, J. Gallagher³⁹, E. Ganster¹, A. Garcia¹⁴, L. Gerhardt⁹, A. Ghadimi⁵⁸, C. Glaser⁶¹, T. Glauch²⁷, T. Glüsenskamp^{26, 61}, N. Goehle³², J. G. Gonzalez⁴⁴, S. Goswami⁵⁸, D. Grant²⁴, S. J. Gray¹⁹, O. Gries¹, S. Griffin⁴⁰, S. Griswold⁵², K. M. Groth²², C. Günther¹, P. Gutjahr²³, C. Haack²⁶, A. Hallgren⁶¹, R. Halliday²⁴, L. Halve¹, F. Halzen⁴⁰, H. Hamdaoui⁵⁵, M. Ha Minh²⁷, K. Hanson⁴⁰, J. Hardin¹⁵, A. A. Harnisch²⁴, P. Hatch³³, A. Haungs³¹, K. Helbing⁶², J. Hellrung¹¹, F. Henningsen²⁷, L. Heuermann¹, N. Heyer⁶¹, S. Hickford⁶², A. Hidvegi⁵⁴, C. Hill¹⁶, G. C. Hill², K. D. Hoffman¹⁹, S. Hori⁴⁰, K. Hoshina^{40, 66}, W. Hou³¹, T. Huber³¹, K. Hultqvist⁵⁴, M. Hünnefeld²³, R. Hussain⁴⁰, K. Hyon²³, S. In⁵⁶, A. Ishihara¹⁶, M. Jacquart⁴⁰, O. Janik¹, M. Jansson⁵⁴, G. S. Japaridze⁵, M. Jeong⁵⁶, M. Jin¹⁴, B. J. P. Jones⁴, D. Kang³¹, W. Kang⁵⁶, X. Kang⁴⁹, A. Kappes⁴³, D. Kappesser⁴¹, L. Kardum²³, T. Karg⁶³, M. Kar²⁷, A. Karle⁴⁰, T. Katori⁶⁷, U. Katz²⁶, M. Kauer⁴⁰, J. L. Kelley⁴⁰, A. Khattee Zathul⁴⁰, A. Kheirandish^{34, 35}, J. Kiriyluk⁵⁵, S. R. Klein^{8, 9}, A. Kochocki²⁴, R. Koirala⁴⁴, H. Kolanoski¹⁰, T. Kontrimas²⁷, L. Köpke⁴¹, C. Kopper²⁶, D. J. Koskinen²², P. Koundal³¹, M. Kovacevich⁴⁹, M. Kowalski^{10, 63}, T. Kozynets²², J. Krishnamoorthi^{40, 64}, K. Kruiswijk³⁷, E. Krupczak²⁴, A. Kumar⁶³, E. Kun¹¹, N. Kurahashi⁴⁹, N. Lad⁶³, C. Lagunas Gualda⁶³, M. Lamoureux³⁷, M. J. Larson¹⁹, S. Latseva¹, F. Lauber⁶², J. P. Lazar^{14, 40}, J. W. Lee⁵⁶, K. Leonard DeHolton⁶⁰, A. Leszczyńska⁴⁴, M. Lincetto¹¹, Q. R. Liu⁴⁰, M. Liubarska²⁵, E. Lohfink⁴¹, C. Love⁴⁹, C. J. Lozano Mariscal⁴³, L. Lu⁴⁰, F. Lucarelli²⁸, W. Luszczyk^{20, 21}, Y. Lyu^{8, 9}, J. Madsen⁴⁰, K. B. M. Mahn²⁴, Y. Makino⁴⁰, E. Manao²⁷, S. Mancina^{40, 48}, S. Mandalia⁶⁸, W. Marie Sainte⁴⁰, I. C. Mariş², S. Marka⁴⁶, Z. Marka⁴⁶, M. Marsee⁵⁸, I. Martinez-Soler¹⁴, R. Maruyama⁴⁵, F. Mayhew²⁴, T. McElroy²⁵, F. McNally³⁸, J. V. Mead²², K. Meagher⁴⁰, S. Mechbal⁶³, A. Medina²¹, M. Meier¹⁶, Y. Merckx¹³, L. Merten¹¹, J. Micallef²⁴, J. Mitchell⁷, T. Montaruli²⁸, R. W. Moore²⁵, Y. Morii¹⁶, R. Morse⁴⁰, M. Moulai⁴⁰, T. Mukherjee³¹, R. Naab⁶³, R. Nagai¹⁶, M. Nakos⁴⁰, U. Naumann⁶², J. Necker⁶³, A. Negi⁴, M. Neumann⁴³, H. Niederhausen²⁴, M. U. Nisa²⁴, A. Noell¹, A. Novikov⁴⁴, S. C. Nowicki²⁴, A. Obertacke Pollmann¹⁶, V. O'Dell⁴⁰, M. Oehler³¹, B. Oeyen²⁹, A. Olivas¹⁹, R. Ørsøe²⁷, J. Osborn⁴⁰, E. O'Sullivan⁶¹, H. Pandya⁴⁴, N. Park³³, G. K. Parker⁴, E. N. Paudel⁴⁴, L. Paul^{42, 50}, C. Pérez de los Heros⁶¹, J. Peterson⁴⁰, S. Philippen¹, A. Pizzuto⁴⁰, M. Plum⁵⁰, A. Pontén⁶¹, Y. Popovych⁴¹, M. Prado Rodriguez⁴⁰, B. Pries²⁴, R. Procter-Murphy¹⁹, G. T. Przybylski⁹, C. Raab³⁷, J. Riedel⁴⁰, K. Rawlins³, Z. Rechac⁴⁰, A. Rehman⁴⁴, P. Reichherzer¹¹, G. Renzi¹², E. Resconi²⁷, S. Reusch⁶³, W. Rhode²³, B. Riedel⁴⁰, A. Rifaie¹, E. J. Roberts², S. Robertson^{8, 9}, S. Rodan⁵⁶, G. Roellinghoff⁵⁶, M. Rongen²⁶, C. Rott^{53, 56}, T. Ruhe²³, L. Ruohan²⁷, D. Ryckbosch²⁹, I. Safa^{14, 40}, J. Saffer³², D. Salazar-Gallegos²⁴, P. Sampathkumar³¹, S. E. Sanchez Herrera²⁴, A. Sandrock⁶², M. Santander⁵⁸, S. Sarkar²⁵, S. Sarkar⁴⁷, J. Savelberg¹, P. Savina⁴⁰, M. Schaufel¹, H. Schieler³¹, S. Schindler²⁶, L. Schlickmann¹, B. Schlüter⁴³, F. Schlüter¹², N. Schmeisser⁶², T. Schmidt¹⁹, J. Schneider²⁶, F. G. Schröder^{31, 44}, L. Schumacher²⁶, G. Schwefer¹, S. Sclafani¹⁹, D. Seckel⁴⁴, M. Seikh³⁶, S. Seunarine⁵¹, R. Shah⁴⁹, A. Sharma⁶¹, S. Shefali³², N. Shimizu¹⁶, M. Silva⁴⁰, B. Skrzypek¹⁴, B. Smithers⁴, R. Snihur⁴⁰, J. Soedingrekso²³, A. Sogaard²², D. Soldin³², P. Soldin¹, G. Sommani¹¹, C. Spannfellner²⁷, G. M. Spiczak⁵¹, C. Spiering⁶³, M. Stamatikos²¹, T. Stanev⁴⁴, T. Stetzelberger⁹, T. Stürwald⁶², T. Stuttard²², G. W. Sullivan¹⁹, I. Taboada⁶, S. Ter-Antonyan⁷, M. Thiesmeyer¹, W. G. Thompson¹⁴, J. Thwaites⁴⁰, S. Tilav⁴⁴, K. Tollefson²⁴, C. Tönnis⁵⁶, S. Toscano¹², D. Tosi⁴⁰, A. Trettin⁶³, C. F. Tung⁶, R. Turcotte³¹, J. P. Twagirayezu²⁴, B. Ty⁴⁰, M. A. Unland Elorrieta⁴³, A. K. Upadhyay^{40, 64}, K. Uphaw⁷, N. Valtonen-Mattila⁶¹, J. Vandenbroucke⁴⁰, N. van Eijndhoven¹³, D. Vannerom¹⁵, J. van Santen⁶³, J. Vara⁴³, J. Veitch-Michaelis⁴⁰, M. Venugopal³¹, M. Vereecken³⁷, S. Verpoest⁴⁴, D. Veske⁴⁶, A. Vijai¹⁹, C. Walck⁵⁴, C. Weaver²⁴, P. Weigel¹⁵, A. Weindl³¹, J. Weldert⁶⁰, C. Wendt⁴⁰, J. Werthebach²³, M. Weyrauch³¹, N. Whitehorn²⁴, C. H. Wiebusch¹, N. Willey²⁴, D. R. Williams⁵⁸, L. Witthaus²³, A. Wolf¹, M. Wolf²⁷, G. Wrede²⁶, X. W. Xu⁷, J. P. Yanez²⁵, E. Yildizci⁴⁰, S. Yoshida¹⁶, R. Young³⁶, F. Yu¹⁴, S. Yu²⁴, T. Yuan⁴⁰, Z. Zhang⁵⁵, P. Zhelnin¹⁴, M. Zimmerman⁴⁰

¹ III. Physikalisches Institut, RWTH Aachen University, D-52056 Aachen, Germany

² Department of Physics, University of Adelaide, Adelaide, 5005, Australia

³ Dept. of Physics and Astronomy, University of Alaska Anchorage, 3211 Providence Dr., Anchorage, AK 99508, USA

⁴ Dept. of Physics, University of Texas at Arlington, 502 Yates St., Science Hall Rm 108, Box 19059, Arlington, TX 76019, USA

⁵ CTSPS, Clark-Atlanta University, Atlanta, GA 30314, USA

⁶ School of Physics and Center for Relativistic Astrophysics, Georgia Institute of Technology, Atlanta, GA 30332, USA

⁷ Dept. of Physics, Southern University, Baton Rouge, LA 70813, USA

⁸ Dept. of Physics, University of California, Berkeley, CA 94720, USA

⁹ Lawrence Berkeley National Laboratory, Berkeley, CA 94720, USA

¹⁰ Institut für Physik, Humboldt-Universität zu Berlin, D-12489 Berlin, Germany

¹¹ Fakultät für Physik & Astronomie, Ruhr-Universität Bochum, D-44780 Bochum, Germany

¹² Université Libre de Bruxelles, Science Faculty CP230, B-1050 Brussels, Belgium

- ¹³ Vrije Universiteit Brussel (VUB), Dienst ELEM, B-1050 Brussels, Belgium
- ¹⁴ Department of Physics and Laboratory for Particle Physics and Cosmology, Harvard University, Cambridge, MA 02138, USA
- ¹⁵ Dept. of Physics, Massachusetts Institute of Technology, Cambridge, MA 02139, USA
- ¹⁶ Dept. of Physics and The International Center for Hadron Astrophysics, Chiba University, Chiba 263-8522, Japan
- ¹⁷ Department of Physics, Loyola University Chicago, Chicago, IL 60660, USA
- ¹⁸ Dept. of Physics and Astronomy, University of Canterbury, Private Bag 4800, Christchurch, New Zealand
- ¹⁹ Dept. of Physics, University of Maryland, College Park, MD 20742, USA
- ²⁰ Dept. of Astronomy, Ohio State University, Columbus, OH 43210, USA
- ²¹ Dept. of Physics and Center for Cosmology and Astro-Particle Physics, Ohio State University, Columbus, OH 43210, USA
- ²² Niels Bohr Institute, University of Copenhagen, DK-2100 Copenhagen, Denmark
- ²³ Dept. of Physics, TU Dortmund University, D-44221 Dortmund, Germany
- ²⁴ Dept. of Physics and Astronomy, Michigan State University, East Lansing, MI 48824, USA
- ²⁵ Dept. of Physics, University of Alberta, Edmonton, Alberta, Canada T6G 2E1
- ²⁶ Erlangen Centre for Astroparticle Physics, Friedrich-Alexander-Universität Erlangen-Nürnberg, D-91058 Erlangen, Germany
- ²⁷ Technical University of Munich, TUM School of Natural Sciences, Department of Physics, D-85748 Garching bei München, Germany
- ²⁸ Département de physique nucléaire et corpusculaire, Université de Genève, CH-1211 Genève, Switzerland
- ²⁹ Dept. of Physics and Astronomy, University of Gent, B-9000 Gent, Belgium
- ³⁰ Dept. of Physics and Astronomy, University of California, Irvine, CA 92697, USA
- ³¹ Karlsruhe Institute of Technology, Institute for Astroparticle Physics, D-76021 Karlsruhe, Germany
- ³² Karlsruhe Institute of Technology, Institute of Experimental Particle Physics, D-76021 Karlsruhe, Germany
- ³³ Dept. of Physics, Engineering Physics, and Astronomy, Queen's University, Kingston, ON K7L 3N6, Canada
- ³⁴ Department of Physics & Astronomy, University of Nevada, Las Vegas, NV, 89154, USA
- ³⁵ Nevada Center for Astrophysics, University of Nevada, Las Vegas, NV 89154, USA
- ³⁶ Dept. of Physics and Astronomy, University of Kansas, Lawrence, KS 66045, USA
- ³⁷ Centre for Cosmology, Particle Physics and Phenomenology - CP3, Université catholique de Louvain, Louvain-la-Neuve, Belgium
- ³⁸ Department of Physics, Mercer University, Macon, GA 31207-0001, USA
- ³⁹ Dept. of Astronomy, University of Wisconsin–Madison, Madison, WI 53706, USA
- ⁴⁰ Dept. of Physics and Wisconsin IceCube Particle Astrophysics Center, University of Wisconsin–Madison, Madison, WI 53706, USA
- ⁴¹ Institute of Physics, University of Mainz, Staudinger Weg 7, D-55099 Mainz, Germany
- ⁴² Department of Physics, Marquette University, Milwaukee, WI, 53201, USA
- ⁴³ Institut für Kernphysik, Westfälische Wilhelms-Universität Münster, D-48149 Münster, Germany
- ⁴⁴ Bartol Research Institute and Dept. of Physics and Astronomy, University of Delaware, Newark, DE 19716, USA
- ⁴⁵ Dept. of Physics, Yale University, New Haven, CT 06520, USA
- ⁴⁶ Columbia Astrophysics and Nevis Laboratories, Columbia University, New York, NY 10027, USA
- ⁴⁷ Dept. of Physics, University of Oxford, Parks Road, Oxford OX1 3PU, United Kingdom
- ⁴⁸ Dipartimento di Fisica e Astronomia Galileo Galilei, Università Degli Studi di Padova, 35122 Padova PD, Italy
- ⁴⁹ Dept. of Physics, Drexel University, 3141 Chestnut Street, Philadelphia, PA 19104, USA
- ⁵⁰ Physics Department, South Dakota School of Mines and Technology, Rapid City, SD 57701, USA
- ⁵¹ Dept. of Physics, University of Wisconsin, River Falls, WI 54022, USA
- ⁵² Dept. of Physics and Astronomy, University of Rochester, Rochester, NY 14627, USA
- ⁵³ Department of Physics and Astronomy, University of Utah, Salt Lake City, UT 84112, USA
- ⁵⁴ Oskar Klein Centre and Dept. of Physics, Stockholm University, SE-10691 Stockholm, Sweden
- ⁵⁵ Dept. of Physics and Astronomy, Stony Brook University, Stony Brook, NY 11794-3800, USA
- ⁵⁶ Dept. of Physics, Sungkyunkwan University, Suwon 16419, Korea
- ⁵⁷ Institute of Physics, Academia Sinica, Taipei, 11529, Taiwan
- ⁵⁸ Dept. of Physics and Astronomy, University of Alabama, Tuscaloosa, AL 35487, USA
- ⁵⁹ Dept. of Astronomy and Astrophysics, Pennsylvania State University, University Park, PA 16802, USA
- ⁶⁰ Dept. of Physics, Pennsylvania State University, University Park, PA 16802, USA
- ⁶¹ Dept. of Physics and Astronomy, Uppsala University, Box 516, S-75120 Uppsala, Sweden
- ⁶² Dept. of Physics, University of Wuppertal, D-42119 Wuppertal, Germany
- ⁶³ Deutsches Elektronen-Synchrotron DESY, Platanenallee 6, 15738 Zeuthen, Germany
- ⁶⁴ Institute of Physics, Sachivalaya Marg, Sainik School Post, Bhubaneswar 751005, India
- ⁶⁵ Department of Space, Earth and Environment, Chalmers University of Technology, 412 96 Gothenburg, Sweden
- ⁶⁶ Earthquake Research Institute, University of Tokyo, Bunkyo, Tokyo 113-0032, Japan
- ⁶⁷ Dept. of Physics, King's College London, London WC2R 2LS, United Kingdom
- ⁶⁸ School of Physics and Astronomy, Queen Mary University of London, London E1 4NS, United Kingdom

Acknowledgements

The authors gratefully acknowledge the support from the following agencies and institutions: USA – U.S. National Science Foundation-Office of Polar Programs, U.S. National Science Foundation-Physics Division, U.S. National Science Foundation-EPSCoR, Wisconsin Alumni Research Foundation, Center for High Throughput Computing (CHTC) at the University of Wisconsin-Madison, Open Science Grid (OSG), Advanced Cyberinfrastructure Coordination Ecosystem: Services & Support (ACCESS), Frontera computing project at the Texas Advanced Computing Center, U.S. Department of Energy-National Energy Research Scientific Computing Center, Particle astrophysics research computing center at the University of Maryland, Institute for Cyber-Enabled Research at Michigan State University, and Astroparticle physics computational facility at Marquette University; Belgium – Funds for Scientific Research (FRS-FNRS and FWO), FWO Odysseus and Big Science programmes, and Belgian Federal Science Policy Office (Belspo); Germany – Bundesministerium für Bildung und Forschung (BMBF), Deutsche Forschungsgemeinschaft (DFG), Helmholtz Alliance for Astroparticle Physics (HAP), Initiative and Networking Fund of the Helmholtz Association, Deutsches Elektronen Synchrotron (DESY), and High Performance Computing cluster of the RWTH Aachen; Sweden – Swedish Research Council, Swedish Polar Research Secretariat, Swedish National Infrastructure for Computing (SNIC), and Knut and Alice Wallenberg Foundation; European Union – EGI Advanced Computing for research; Australia – Australian Research Council; Canada – Natural Sciences and Engineering Research Council of Canada, Calcul Québec, Compute Ontario, Canada Foundation for Innovation, WestGrid, and Compute Canada; Denmark – Villum Fonden, Carlsberg Foundation, and European Commission; New Zealand – Marsden Fund; Japan – Japan Society for Promotion of Science (JSPS) and Institute for Global Prominent Research (IGPR) of Chiba University; Korea – National Research Foundation of Korea (NRF); Switzerland – Swiss National Science Foundation (SNSF); United Kingdom – Science and Technology Facilities Council (STFC) and Department of Physics, University of Oxford.